Glutathione peroxidase 3 (GPX3) expression predicts the prognosis of numerous malignant tumors: A pan-cancer Analysis

Yuetong Wang
Shaanxi Academy of Traditional Chinese Medicine
Guotao Fu
Shaanxi University of Chinese Medicine
Xueqin Chen
Shaanxi University of Chinese Medicine
Zengrun Xia
Ankang R&D Center of Se-enriched Products
Meng Qi
Ankang R&D Center of Se-enriched Products
Xiaoping Du
Ankang R&D Center of Se-enriched Products
Kun Liu
Binzhou Medical University
Qiling Liu
Shaanxi University of Chinese Medicine
Na Sun
Shaanxi University of Chinese Medicine
Chuandao Shi
Shaanxi University of Chinese Medicine
Rongqiang Zhang (Zhangrqxianyang@163.com)
Shaanxi University of Chinese Medicine
Kai Qu
Shaanxi Provincial Hospital of Chinese Medicine

Research

Keywords: Gene expression, Glutathione peroxidase 3 (GPX3), Tumors, Biomarkers

Posted Date: October 15th, 2021

DOI: https://doi.org/10.21203/rs.3.rs-845660/v2

Abstract

Background

Malignant tumor is a general term for uncontrollable growth of cells. Several studies have investigated that role of *GPX3* in tumors. However, no pan-cancer analysis has be conducted to assess the diagnostic and prognostic potential of *GPX3*.

Methods

GPX3 mRNA and protein expression profile was analyzed in the TCGA + GTEx database and CPTAC database. Kaplan-Meier survival curves and forest plots were constructed to help evaluate the impact of *GPX3* on the survival and prognosis of cancer patients. Gene mutations of *GPX3* were analyzed based on TMB/MSI. The correlation between *GPX3* and tumor immune infiltration was assessed using TIMER2. Enrichment analysis was performed to determine tumor-related signaling pathways associated with *GPX3*. A prediction model for STAD was established.

Results

GPX3 was downregulated in most malignant tumors, and was significantly associated with the survival and prognosis of malignant tumors, such as STAD, PAAD, COAD, etc. Moreover, *GPX3* expression was positively correlated and negatively with MSI in 13 and 20 categories of tumor respectively after *GPX3* expression was positively correlated and negatively with TMB in 9 and 24 tumors separately ($P < 0.05$). A positive correlation was found between *GPX3* and the infiltration level of major immune cells and Cancer-associated fibroblasts ($P < 0.05$). The effects of *GPX3* were mediated by the AMPK signaling pathway, fructose and mannose metabolism.

Conclusions

This is a novel pan-cancer analysis on the relationship between *GPX3* and human tumors. Findings of this research will deepen our understanding on the role of *GPX3* in the development, regulation and prognosis of malignant tumors.

1. Background

Malignant tumor is a general term for uncontrollable growth of cells. Here, cells do not respond to normal regulatory signals, grows and differentiates abnormally and display local tissue invasion and distant metastasis [1]. There are currently about 260 types of tumors in humans. According to the latest global cancer statistics by the World Health Organization, in 2020 alone, there were 19.29 million new cancer cases worldwide, resulting in 9.96 million deaths [2]. Cancers present a huge economic burden to patients, their families and even the nation, threatening both social and economic development. Cancer is highly fatal and seriously threatens human health and life. Even with the recent advances in diagnosis and treatment, the occurrence and mortality due to of malignant tumors are still increasing. Biomarkers are potentially accurate and effective diagnostic and therapeutic targets for malignant tumors.

Glutathione peroxidase (*GPX*) is an important protein that scavenges reactive oxygen species (ROS) in organisms [3]. Glutathione peroxidase 3 (*GPX3*) is the only known extracellular glycosylase in the glutathione peroxidase family and contains the selenocysteine residues. It defends against cellular stress signals and reactive oxygen species, thereby maintaining the cellular genetic integrity [4]. Moderate *GPX3* expression is necessary to maintain normal metabolism and physiology and induction of important pathological changes in certain organs. However, abnormal expression of *GPX3* results in the occurrence and development of various malignant tumors in the body. For instance, recent researches have demonstrated the abnormal expression of *GPX3* in esophageal cancer [5], melanoma [6], colon cancer [7], gastric cancer [8], ovarian cancer [9] and other malignant tumors. Even so, studies on the role of *GPX3* are relatively few and have only assessed the role of *GPX3* in a small number of malignant tumors.

Pan-Cancer Analysis Project is a collaborative initiative that integrates, analyzes and interprets The Cancer Genome Atlas (TCGA) data of different malignant tumors from different platforms [10,11]. Pan-cancer analyses can not only reveal common phenotypic characteristics of malignant tumors, but can also unravel molecular events underlying the development of tumors and corresponding internal regulatory mechanisms. These studies are also important in unraveling the complex tumorigenesis as well as possible molecular and target genes relevant to clinical prognosis of cancers. However, even with the large amount of clinical data, there is no pan-cancer evidence on the relationship between *GPX3* and several tumor types.

Herein, we first analyzed the expression of *GPX3* in 33 different malignant tumors using RNA-seq data. Then we analyzed the correlation between *GPX3* expression and tumor stage. The effect of *GPX3* on the survival and prognosis of malignant tumor was also investigated. We explored the relationship between *GPX3* expression and infiltration of immune cells. we also performed bioinformatics analyses to explore potential mechanism underlying *GPX3* expression and development of human malignant tumors. Finally, we verified the expression pattern and prognostic significance of *GPX3* in STAD and COAD, and proposed a prediction model for STAD. Findings of this research will deepen our understanding on the role of *GPX3* in the development, regulation and prognosis of malignant tumors. It can also uncover potential biomarkers for early diagnosis, prevention and treatment of malignant tumors.

2. Materials And Methods

2.1 Expression of GPX3 in normal human tissues

The Human Protein Atlas (HPA) (https://www.proteinatlas.org/) is a comprehensive repository for protein expression profiles in tissue, cells and blood and their metabolic and pathologic roles in the body. The expression of *GPX3* in normal tissues was analyzed using HPA RNA-seq tissue data [12]. The expression of GPX3 protein in main cancer tissues (Colorectal cancer, Prostate cancer, Breast cancer, Lung cancer, Liver cancer) and normal tissues (Normal kidney tissues) was analyzed using immunohistochemical (IHC) tissue images in HPA.

2.2 Gene expression analysis

The expression of *GPX3* mRNA in 33 different malignant tumors and corresponding normal tissues was assessed using RNA sequence data in the TCGA and GTEx databases [13]. Differential gene expression between cancerous and corresponding normal tissues was analyzed using t-tests, whereas the differently expressed genes between

the tissue sets were presented using a violin plot. Before plotting, the expression data was first transformed to log2 [TPM (Transcripts per million) + 1], with $P < 0.05$ considered statistically significant.

The cancer omics data from the Clinical proteomic tumor analysis consortium (CPTAC) was analyzed using UALCAN platform (http://ualcan.path.uab.edu/analysis-prot.html) [14]. The major analysis involved the expression of *GPX3* several malignant tumors including Breast cancer, Ovarian cancer, Colon cancer, Clear cell Renal Cell Carcinoma (Clear cell RCC), Uterine Corpus Endometrial Carcinoma (UCEC) and Lung adenocarcinoma (LUAD). The degree and nature of abnormal expression of *GPX3* protein between cancer and adjacent normal tissues was based on Z-values, with the median protein expression levels used as reference points.

The *GPX3* expression at different cancer stages was analyzed using the "Expression DIY" module in GEPIA2 platform (http://gepia2.cancer-pku.cn/#index). The corresponding violin plot was also constructed after transformation of the expression data to $\log_2$ (TPM + 1). The comparative analyses for the expression of *GPX3* in different cancer stages were performed to understand the role of the protein in cancer pathology [15].

2.3 Prognostic utility of *GPX3*

We constructed the predictive potential of *GPX3* for Overall Survival (OS), Disease Specific Survival (DSS), Disease-Free Interval (DFI) and Progression-Free Interval (PFI) of different tumors in the TCGA database. The median *GPX3* expression was used as the cutoff level for high and low expression of the protein. The predictive utility of *GPX3* for OS, DSS, DFI and PFI of cancer patients was assessed using log-rank test and the Kaplan-Meier curve.

Further analyses were performed to assess epidemiological implication of *GPX3* expression in 33 tumor types in the TCGA database. The effect of *GPX3* expression on Overall Survival (OS), Disease-Free Survival (DFS), Progression Free Survival (PFS) and Disease Specific Survival (DSS) for different cancers were assessed using R software V. 4.0.3. The relationship between *GPX3* expression and OS, DFS, PFS and DSS were analyzed using univariate Cox regression analysis and hazard ratios (HR) at 95% confidence interval (CI) and log-rank *P* test at statistical significance of $P < 0.05$ [16].

2.4 Genetic alteration in tumor cells

RNA-seq data for 33 cancer patients in TCGA database were downloaded from the genomic data Commons (GDC) portal (https://portal.gdc.cancer.gov/). Tumor Mutation Burden (TMB), defined as the number of mutations (insertion/deletion) per mega base in the exon coding region of a gene, was analyzed as previously described [17]. The TMB is directly proportional to the expression of neoantigens recognizable by T cells, which influences the immune response. Microsatellite Instability (MSI) is any change in the microsatellite length caused by insertion or deletion of a repeat unit in a gene in a tumor tissue, relative to normal tissue [18], which generates microsatellite alleles. TMB and MSI are often used in assessing the prognosis and effect of immunotherapies. The association between *GPX3* expression and TMB and MSI in cancerous tissues was assessed. Relevant data was obtained from the TCGA database; whereas the analysis was performed using R software V. 4.0.3, with statistical significance sets at $P < 0.05$.

2.5 Infiltration of immune cells

Tumor Immune Evaluation Resource 2 (TIMER2) is a database for the systematic analysis of immune infiltration of different cancer types (B cells, CD4 + T cells, CD8 + T cells, Neutrophils, Macrophages, and Dendritic cells). In

this study, infiltrating immune cell scores of 33 cancers were downloaded from the TIMER2 database. Spearman correlation analysis was used to evaluate the correlation between *GPX3* expression and scores of B cells, CD4 + T cells, CD8 + T cells, Neutrophils, Macrophages, and Dendritic cells [19].

The relationship between *GPX3* expression and infiltration levels of Cancer associated fibroblasts (CAFs) was analyzed using TIMER2 platform (http://timer.cistrome.org/). CAF regulates functioning of immune cells in the tumor microenvironment (TME). The infiltration of immune cells in the TME were estimated using EPIC, MCPCOUNTER, XCELL and TIDE algorithms. Since most immune cell types are negatively correlated with tumor purity, we obtained *P*-values and correlation coefficient by Spearman's rank correlation test after purity adjustment. The above relationship was presented using a heat map and a scatter plot. Scatter plot was constructed for cells exhibiting the strongest correlation with tumor ($P < 0.05$).[15]

2.6 Enrichment analysis

The top 100 genes associated with *GPX3* expression in TCGA and GTEx databases were identified based on Pearson's correlation coefficient (PCC). The correlations between *GPX3* and the top 3 most dysregulated genes were also assessed using GEPIA2 module. A scatter plot for the top 3 most dysregulated genes was also constructed.

Protein-protein interaction (PPI) network in tumor tissues associated with *GPX3* expression was constructed using STRING platform (https://string-db.org/). The minimum required interaction score was set as Low confidence = 0.150, the max number of interactors to show was set as no more than 50 interactors in 1st shell. Finally, the available experimentally determined GPX3-binding proteins were obtained.

KEGG (Kyoto Encyclopedia of Genes and Genomes) pathway enrichment analysis of the 150 genes, which was combined from top 100 GPX3-similar genes and 50 GPX3-interacted genes, was performed to identify pathways regulated by the proteins. The resultant genes were uploaded to DAVID database, under the name of ("OFFICIAL_GENE_SYMBOL") and ("Homo sapiens") for species. GO (Gene Ontology) enrichment analysis for the Biological Process (BP), Cellular Component (CC) and Molecular Function (MF) associated with the dysregulated genes were also identified and plotted graphically using the cnetplot package (circular = F, colorEdge = T, node_label = T). KEGG and GO analyses were performed using R software. Statistical significance for both analyses was set at two-tailed $P < 0.05$ [15].

2.7 Construction and validation of the nomogram of *GPX3* for STAD

The results above indicated that *GPX3* expression had an important impact on the survival prognosis of numerous malignant tumors, such as BLCA, COAD, PAAD, STAD. OS, DSS, PFS, DFS, DFI and PFI all strongly supported that the prognosis of STAD would get worse when *GPX3* level elevated. Therefore, a nomogram of *GPX3* for STAD was established and verified to further analyze the predictive significance of *GPX3* for the OS of patients with STAD. Firstly, univariate and multivariate Cox regression analysis were used to identify all independent factors for STAD and displayed as hazard ratios (HR) combined with the corresponding 95% confidence intervals (CI). Then, according to the results of the multivariate Cox regression analysis model, a prognostic nomogram was established to predict the OS probability of STAD patients at 1-, 2-, 3-, and 5-year by the TCGA training dataset by using the rms package in R software. Concordance index (C-index), which ranges from 0.5 (poor) to 1.0 (perfect), was employed to assess the performance of nomogram. Briefly, the higher the C-

index, the better its prognostic accuracy. Finally, to ensure the nomograms' accuracy, calibration and validation of the nomogram were performed using the R package "rms" and "cmprsk", $P < 0.05$ was considered statistically significant [20, 21].

3 Results

3.1 Expression of *GPX3* in normal human tissues

GPX3 gene is strongly expressed in Kidney, Thyroid gland and Adipose tissues, etc. (Fig. 1A). GPX3 protein was detected in carcinoid, colorectal cancer, prostate cancer, renal cancer, skin cancer and lymphomas (Fig. 1B). The IHC images for GPX3 protein in colorectal cancer, prostate cancer, breast cancer, lung cancer, liver cancer and normal kidney tissues are shown in Fig. 1C-H. Detailed clinical information of the tissue donors for IHC analyses are summarized in Table 1.

Table 1
Key clinical information of subjects for immunohistochemical experiment

Protein	Tissue		Histological type	Age	Gender	Location	Quantity	Intensity
GPX3	Colorectal		Adenocarcinoma	78	female	Cytoplasmic/ membranous nuclear	> 75%	Moderate
GPX3	Breast		Duct carcinoma	61	female	Cytoplasmic/ membranous	> 75%	Weak
GPX3	Prostate		Adenocarcinoma	68	male	Cytoplasmic/ membranous	< 25%	Strong
GPX3	Lung		Squamous cell carcinoma	64	male	Nuclear	< 25%	Weak
GPX3	Liver		Carcinoma/ Hepatocellular	73	female	Cytoplasmic/ membranous	< 25%	Moderate
GPX3	Kidney	glomeruli	Normal tissues	61	male	Cytoplasmic/	< 25%	Weak
		tubules				Membranous nuclear	> 75%	Strong

3.2 *GPX3* gene expression in different tumors

Analysis of data in TCGA and GTEx databases revealed that *GPX3* gene was under expressed in 22 of 34 tumor types including Adrenocortical carcinoma (ACC), Bladder Urothelial Carcinoma (BLCA), Breast invasive carcinoma (BRCA), Cervical squamous cell carcinoma and endocervical adenocarcinoma (CESC), Cholangiocarcinoma (CHOL), Colon adenocarcinoma (COAD), Esophageal carcinoma (ESCA), Head and Neck squamous cell carcinoma (HNSC), Kidney Chromophobe (KICH), Kidney renal clear cell carcinoma (KIRC), Kidney renal papillary cell carcinoma (KIRP), Lung adenocarcinoma (LUAD), Lung squamous cell carcinoma (LUSC), Ovarian serous cystadenocarcinoma (OV), Prostate adenocarcinoma (PRAD), Rectum adenocarcinoma (READ), Skin Cutaneous

Melanoma (SKCM), Stomach adenocarcinoma (STAD), Testicular Germ Cell Tumors (TGCT), Thyroid carcinoma (THCA), Uterine Corpus Endometrial Carcinoma (UCEC) and Uterine Carcinosarcoma (UCS). Among them, analyses were performed at statistical significance of $P < 0.01$ for CHOL and $P < 0.001$ for the rest of the tumors. Expression of *GPX3* gene was relatively higher Lymphoid Neoplasm Diffuse Large B-cell Lymphoma (DLBC), Glioblastoma multiforme (GBM), Glioma (LGG), Liver hepatocellular carcinoma (LIHC) (all at $P < 0.001$) (Fig. 2).

As shown in Fig. 3A, analysis of CPTAC data revealed that compared with normal tissues, *GPX3* was under expressed in Breast cancer, Ovarian cancer, Colon cancer, Clear cell RCC, UCEC, and Lung adenocarcinoma ($P < 0.001$).

Further analyses revealed that *GPX3* expression levels correlated with pathological stages of eight cancers including ACC, BLCA, KIRC, KIRP, LIHC, Pancreatic adenocarcinoma (PAAD), READ and THCA (all at $P < 0.05$) (Fig. 3B). The expression of *GPX3* was highest in stage I and lowest in stage II of ACC. In BLCA, *GPX3* expression was highest in stage III, lowest in stage II and moderate in stage IV. There were no significance differences in *GPX3* expression between stage I and III of KIRC, the same as stage II and IV. In KIRP, *GPX3* expression increased gradually between stage I-III but decreased slightly in stage IV. In LIHC, *GPX3* expression was highest in stage IV and lowest in stage III, In PAAD, *GPX3* expression was highest in stage III and lowest in stage II whereas in READ, *GPX3* expression increased from stage I to stage IV. In THCA, *GPX3* expression was highest in stage II but lowest in stage IV.

3.3 Prognostic value of *GPX3*

Cancer patients were divided into high and low *GPX3* expression groups. The *GPX3* expression predicted the OS of four tumor types. Among them, high *GPX3* expression conferred longer OS of patients with PAAD ($P = 0.0031$), whereas low *GPX3* expression was linked to longer OS of patients with BLCA ($P = 0.0049$), COAD ($P = 0.0078$) and STAD ($P = 0.00041$) (Fig. 4A). The *GPX3* expression also predicted the DSS of four tumor types and high *GPX3* expression conferred longer DSS of patients with PAAD ($P = 0.0091$), whereas low *GPX3* expression was linked to longer DSS of patients with BLCA ($P = 0.1$), COAD ($P = 0.00026$) and STAD ($P = 0.00028$) (Fig. 4B). The *GPX3* expression predicted the DFI of three tumor types. Low *GPX3* expression was linked to longer DFI of patients with BRCA ($P = 0.012$) LUAD ($P = 0.004$) and STAD (P = 0.00016) (Fig. 4C). Meanwhile, high-expression of *GPX3* was associated with longer PFI of PAAD ($P = 0.0037$). Contrarily, low expression of *GPX3* was associated with longer PFI of patients with COAD ($P = 0.0036$) and STAD ($P < 0.0001$) cancers (Fig. 4D).

Univariate survival analysis revealed that high-expression of *GPX3* was related to poor prognosis of STAD (HR = 1.002, 95%CI: 1-1.003, $P = 0.0125$) but better prognosis of PAAD (HR = 0.998, 95%CI: 0.997-1, $P = 0.0134$) (Fig. 5A). Meanwhile, over *GPX3* expression was linked with DFS of COAD (HR = 1.003, 95%CI: 1.001–1.006, $P = 0.0105$), STAD (HR = 1.002, 95%CI: 1.001–1.003, $P = 0.0048$) and PAAD (HR = 0.998, 95%CI: 0.997-1, $P = 0.0067$) (Fig. 5B). Moreover, over-expression of *GPX3* was associated with PFS of patients with COAD (HR = 1.004, 95%CI: 1.001–1.007, $P = 0.0028$), STAD (HR = 1.002, 95%CI: 1-1.003, $P = 0.0151$) and PAAD (HR = 0.998, 95%CI: 0.997-1, $P = 0.0134$) (Fig. 5C). Also, high-expression of *GPX3* was associated with poor prognosis of BRCA (HR = 1.002, 95%CI: 1.001–1.004, $P = 0.0068$) and STAD (HR = 1.003, 95%CI: 1.001–1.006, $P = 0.0069$) but better prognosis of LUAD (HR = 0.998, 95%CI: 0.997-1, $P = 0.0322$) (Fig. 5D).

Overall, these findings demonstrate that *GPX3* expression levels influence the prognosis of several tumors, particular STAD, and COAD PAAD. Therefore, we focused on these 3 types of tumors in subsequent analyses,

especially on STAD, and COAD due to larger sample sizes.

3.4 The correlation between *GPX3* expression and TMB/MSI

GPX3 expression positively correlated with TMB of nine tumor types including THYM, Acute Myeloid Leukemia (LAML), LIHC, KIRC, KIRP, COAD, TGCT, SARC and PCPG. The strongest correlation was observed for THYM, LAML and LIHC. Contrarily, *GPX3* expression negatively correlated with TMB of 24 tumor types including PRAD, PAAD, STAD, SKCM, UCS, ESCA, LUAD, KICH, GBM, LUSC, Uveal Melanoma (UVM), THCA, Mesothelioma (MESO), HNSC, ACC, READ, LGG, BRCA, DLBC, BLCA, OV, CHOL, UCEC and CESC. The strongest correlation was observed for PRAD, PAAD and STAD (Fig. 6A). *GPX3* expression also positively correlated with the MSI of SKCM, COAD, KIRC, BLCA, UCEC, CESC, BRCA, ESCA, THYM, THCA, LAML, READ and MESO. The strongest correlations were observed for SKCM, COAD and KIRC. However, there was a strong negatively correlation between *GPX3* expression and MSI of STAD, CHOL, KICH, OV, LUSC, LUAD, GBM, UCS, Pheochromocytoma and Paraganglioma (PCPG), TGCT, PRAD, ACC, Sarcoma (SARC), HNSC, KIRP, LIHC, LGG, DLBC, PAAD and UVM. The strongest correlations were observed for STAD, CHOL and KICH (all *Ps* < 0.05) (Fig. 6B).

3.5 *GPX3* expression and infiltration of Immune cells

We investigated whether the expression of *GPX3* in 33 tumors from the TIMER2 database was related to the level of immune infiltration. The results showed that the expression of *GPX3* in PAAD and COAD was significantly positively correlated with B cells, CD4 + T cells, CD8 + T cells, Neutrophils, Macrophages and Dendritic cells. In STAD, the expression of *GPX3* was significantly positively correlated with the infiltration levels of CD4 + T cells, CD8 + T cells, Neutrophils, Macrophages and Dendritic cells, but not with B cells (Fig. 7A).

The relationship between *GPX3* expression and infiltration levels of CAFs in the 40 evaluated tumors were assessed using TIDE, XCELL, EPIC and MCPCOUNTER algorithms. We found *GPX3* expression positively correlated with infiltration of CAFs in BLCA, BRCA, BRCA-Basal, BRCA-LumA, BRCA-LumB, COAD, HNSC, HNSC-HPV-, PAAD, READ, SKCM-Metastasis, STAD and Thymoma (THYM). A scatter plot for the above relationships is shown in Fig. 7B. Such as, based on TIDE algorithm, *GPX3* expression positively correlated with the infiltration level of CAFs in BLCA tissues (Rho = 0.394, *P* = 4.17e-15).

3.6 Key pathways linked to *GPX3* expression

Top 3 genes related to *GPX3* expression based on the TCGA data were further analyzed. It was found *GPX3* expression positively correlated with expression of MOCS1 (*R* = 0.28), TNS2 (*R* = 0.2) and FZD4 (*R* = 0.27) genes (Fig. 8A). Further analyses identified 24 *GPX3* binding proteins. The interaction network of these proteins is shown in Fig. 8B. KEGG analyses revealed that the pathogenesis of *GPX3* in tumors was related to AMPK and Fructose and mannose metabolism pathways (Fig. 8C). The GO enrichment analysis further revealed that *GPX3* gene regulates Angiogenesis and vascular morphogenesis, vasculature development, tube morphogenesis among others. The gene also regulates expression of intrinsic components of plasma membrane as well as phosphatase and Phosphoric ester hydrolase activities.

3.7 Validation analysis

In the above prognosis analysis, *GPX3* showed significant effects on STAD, COAD and PAAD, especially on STAD and COAD in OS, DFS, PFS, DFI and PFI. To verify the expression pattern and prognostic significance of *GPX3* in STAD and COAD, we further retrieved two datasets from Gene Expression Omnibus (GEO) (https://www.ncbi.nlm.nih.gov/geo/) and TCGA with the accession numbers GSE44861 and GSE29272 [22, 23].

The results showed that the expression level of *GPX3* in STAD and COAD tumor tissues was significantly lower than that in normal tissues, which were consistent with the results of TCGA datasets. The AUCs (area under the ROC curves) for COAD was 0.6698 (95%CI: 0.5660–0.7736, P=0.002) from GEO dataset and 0.9909 (95%CI: 0.9862–0.9956, P < 0.001) from TCGA dataset (Fig. 9A). The AUCs for STAD was 0.8406 (95%CI: 0.7865–0.8946, P < 0.001) from GEO dataset and 0.9599 (95%CI: 0.9464–0.9734, P < 0.001) from TCGA dataset (Fig. 9B), respectively. The results suggested that the diagnostic values of *GPX3* for STAD and COAD was the same based on GEO and TCGA database, and *GPX3* performed a good diagnosis ability for the two diseases, which also demonstrated that our aforementioned results were reliable.

3.8 Construction and verification of nomogram

Independent prognostic factors, including pTNM stage, age, radiation therapy, and *GPX3* expression were included to create prognostic nomograms for the OS of STAD patients. The nomogram showed that pTNM stage had the greatest influence on prognosis, followed by age and radiation therapy (Fig. 10A-B). In addition, the validation of the nomogram was performed by C-index and calibration. The C-index predicted by the histogram was 0.69 (95%CI: 0.627-1; *P* < 0.001) (Fig. 10C). The calibration curve showed the concordant survival rate between the predicted and observed nomograms (Fig. 10D). It can be believed the prognostic nomogram established in our present study could effectively predict OS probability of patients with STAD.

4. Discussion

Numerous complex multi-step processes precede development of malignant tumors, induced by numerous biological, chemical and physical factors. Recent diagnosis and treatment advances have facilitated early detection and improved overall survival of cancer patients. However, prognosis modalities are still at infancy stage. Understanding molecular mechanism of tumor pathogenesis can potentially improve or provide new frontier in the diagnosis, treatment and prevention of tumors. *GPX3* is a tumor suppressor gene located on chromosome 5q23. It codes for the main antioxidant enzyme in plasma which participates in detoxification of free oxygen radicals such as hydrogen peroxide, thus protecting cells from oxidative stress-induced damage. Inactivation of *GPX3* leads to the accumulation of ROS, which have been found to induce oxidative deoxyribonucleic acid (DNA) damage. The resultant gene changes lead to development of cancers [24]. Lou W et al. [25] reported that *GPX3* participates in the growth and metastasis of breast cancer. In a related study, Noci S et al. [26] found that *GPX3* expression influences the incidence, survival rate and recurrence of colorectal cancer. However, the roles of *GPX3* in different tumor types are still unclear. Moreover, to the best of our knowledge, there is few pan-cancer studies on the role of *GPX3* in various cancer properties. Therefore, we evaluated the role of *GPX3* expression on normal human tissues, gene expression, protein expression, prognosis, gene mutation, infiltration of immune cells, associated pathways, prognostic model, etc. Data for 33 different tumor types was extracted from the TCGA, GTEx, CPTAC, HPA and other databases.

We found *GPX3* expression was modulated in most tumors. In one study, under-expression of *GPX3* was associated with metastasis of thyroid cancer. Moreover, expression levels of *GPX3* corresponded with stage of the cancer [27]. In a related study, [28] under expression of *GPX3* was associated with larger volume, more nodules worse clinical stage and poor prognosis of HCC. Both in vivo and in vitro studies [29] demonstrated that under-expression of *GPX3* participated in the invasion and metastasis of gastric cancer. In this study, we found dysregulated *GPX3* expression in 26 of 33 tumor types. Particularly, *GPX3* expression was downregulated in 22

but up-regulated in 4 of the tumor types. Further analyses revealed under expression of GPX3 protein in all 6 tumors in CPTAC database. We also found *GPX3* expression correlated with pathological stages of tumors. Overall, *GPX3* expression significantly impacts on progression of several tumors.

GPX3 expression levels influences the prognosis of most tumors. However, there are different reports about the role of *GPX3* high / low expression in different tumor prognosis. Several studies have shown that loss of *GPX3* expression in tumor tissues is associated with poor prognosis and chemotherapy resistance in patients [30,31]. Low expression of *GPX3* can also predict patient prognosis. For instance, Caroline C et al. [32] found that under-expression of *GPX3* strongly correlated with low survival rate of lung adenocarcinoma and low-grade gliomas. However, *GPX3* expression was elevated in other tumor tissues [33,34,35], high expression of *GPX3* is associated with poor prognosis in cancer patients such as gastric cancer and lung squamous cell carcinoma. Herein, tumor patients were divided into high and low expression *GPX3* expression groups. We found low-expression of *GPX3* resulted in better prognosis of patients with BLCA, COAD and STAD, but poor prognosis of PAAD. Meanwhile, low-expression of *GPX3* was linked to longer DFI and PFI of patients with BRCA, LUAD, STAD, COAD and STAD but poor PFI of PAAD patients. Further Univariate Cox regression analyses revealed that *GPX3* expression levels predicted the OS, DFS, PFS and DSS of patients with several cancers such as PAAD, STAD, BRCA, LUAD and COAD. It can be concluded that in OS, DFS and PFS, PAAD with low GPX3 expression has a worse prognosis, and COAD and STAD with low *GPX3* expression have a better prognosis. When *GPX3* expression was low in STAD and BRCA, DSS was longer, whereas LUAD was shorter. That is, although Fig. 4 and Fig. 5 were different algorithms, they both illustrate the prognostic value of *GPX3* in different tumors. It can be seen that *GPX3* plays a dichotomy role in different tumor types, both as a tumor suppressor protein and as a survival promoting protein. However, it is necessary to further study the molecular evidence of how the high / low expression of *GPX3* specifically affects the scavenging and redox signals of oxidants in the microenvironment of tumor cells.

This presents the first report of the association between *GPX3* expression and TMB/MSI, and some tumor types that may benefit more from immunotherapy were identified. The potential relationship between infiltration of Immune cell and *GPX3* expression in different tumor types was understood. This study also showed that *GPX3* expression positively correlated with infiltration of CAFs in BLCA, BRCA, BRCA-Basal, etc. Besides, *GPX3*-binding components and *GPX3* expression related genes in all TCGA tumors were integrated for enrichment analysis, and it was found that "AMPK signaling pathway" and "Fructose and mannose metabolism" had an influence on the etiology or pathogenesis of tumors. The nomograms were constructed and validated to provide a prediction of 1-, 2-, 3- and 5-year survival in patients with STAD. It showed good performance in applicability and accuracy, which also supported that the relationship between *GPX3* expression and STAD discovered above. Combined with the existing research results, we speculate that *GPX3* plays an important role in the occurrence and development of STAD, and is expected to become a new target for the diagnosis and treatment of STAD. However, due to the small sample size in this study, more experiments are needed to explore the specific mechanism of *GPX3* in the development of STAD and other cancers.

Conclusion

In summary, the mRNA level of *GPX3* is altered in 26 types of malignant tumors. Specifically, it is upregulated in 4 types of tumors and downregulated in 22 types of tumors, suggesting that the low expression of *GPX3* contributes to the occurrence and development of some tumors. Changes in *GPX3* expression can affect the OS, DFS, PFS, DFI, PFI and DSS of 3 types of tumors. In all TCGA tumors, the potential correlation between *GPX3*

expression and MSI or TMB was proposed for the first time. The expression of *GPX3* in most tumors was positively correlated with the infiltration level of 6 classic immune cells. Meanwhile, the expression of *GPX3* in some tumors is related to the level of immune infiltration of CAFs. *GPX3* participates in tumorigenesis by regulating AMPK signaling pathway. After functional validation and prognostic modeling, *GPX3* was found to be a prognostic marker for STAD. This study provides blueprint data concerning the correlation between *GPX3* and human tumors. The results of this analysis therefore expand our understanding on the role and mechanism of *GPX3* in tumorigenesis.

Abbreviations

GPX
Glutathione peroxidase
ROS
Reactive oxygen species
GPX3
Glutathione peroxidase 3
TCGA
The Cancer Genome Atlas
HPA
Human Protein Atlas
IHC
immunohistochemical
TPM
Transcripts per million
CPTAC
Clinical proteomic tumor analysis consortium
GEO
Gene Expression Omnibus
Clear cell RCC
Clear cell Renal Cell Carcinoma
UCEC
Uterine Corpus Endometrial Carcinoma
LUAD
Lung adenocarcinoma
OS
Overall Survival
DFS
Disease-Free Survival
PFS
Progression Free Survival
DSS
Disease Specific Survival
DFI

Disease-Free Interval
PFI
Progression-Free Interval
HR
hazard ratios
CI
confidence interval
GDC
genomic data Commons
TMB
Tumor Mutation Burden
MSI
Microsatellite Instability
CAFs
Cancer associated fibroblasts
TME
tumor microenvironment
PCC
Pearson’s correlation coefficient
PPI
Protein-protein interaction
KEGG
Kyoto Encyclopedia of Genes and Genomes
GO
Gene Ontology
BP
Biological Process
CC
Cellular Component
MF
Molecular Function
C-index
Concordance index
ACC
Adrenocortical carcinoma
BLCA
Bladder Urothelial Carcinoma
BRCA
Breast invasive carcinoma
CESC
Cervical squamous cell carcinoma and endocervical adenocarcinoma
CHOL
Cholangiocarcinoma, COAD:Colon adenocarcinoma

ESCA
Esophageal carcinoma, HNSC:Head and Neck squamous cell carcinoma
KICH
Kidney Chromophobe
KIRC
Kidney renal clear cell carcinoma
KIRP
Kidney renal papillary cell carcinoma
LUAD
Lung adenocarcinoma
LUSC
Lung squamous cell carcinoma
OV
Ovarian serous cystadenocarcinoma
PRAD
Prostate adenocarcinoma
READ
Rectum adenocarcinoma
SKCM
Skin Cutaneous Melanoma
STAD
Stomach adenocarcinoma
TGCT
Testicular Germ Cell Tumors
THCA
Thyroid carcinoma
UCEC
Uterine Corpus Endometrial Carcinoma
UCS
Uterine Carcinosarcoma
DLBC
Lymphoid Neoplasm Diffuse Large B-cell Lymphoma
GBM
Glioblastoma multiforme
LGG
Glioma
LIHC
Liver hepatocellular carcinoma
PAAD
Pancreatic adenocarcinoma
LAML
Acute Myeloid Leukemia
UVM

Uveal Melanoma
MESO
Mesothelioma
PCPG
Pheochromocytoma and Paraganglioma
SARC
Sarcoma
THYM
Thymoma
AUC
Area Under Curve.

Declarations

Ethical Approval and Consent to Participate

All data for this study are derived from publicly available databases and does not directly involve human participants. Therefore, ethical approval was not required for this article.

Consent for publication

Not relevant.

Availability of data and materials

The TCGA and GTEx data set was obtained from open databases. TCGA data set can be obtained from the following website: http://cancergenome.nih.gov. GTEx data set can be obtained from the following website: http://commonfund.nih.gov/GTEx/.

Competing Interests

The authors declare no conflict of interest.

Funding

This study was supported by Key Research and Development Program in Shaanxi Province (2020SF-076), Research Project from Health Commission of Shaanxi Provincial Government (2018A017), Education Department of Shaanxi Provincial Government (19JS015), Special R&D Program Project of Chinese Academy of Se-enriched Industry (2020FXZX05-01), Chinese Medicine Science and Technology Research Special Project of State Administration of Traditional Chinese Medicine (GZY-KJS-2021-006), National Science Foundation Project (81603454), Clinical collaborative innovation project of integrated traditional Chinese and Western medicine by Shaanxi Administration of traditional Chinese Medicine (2020-ZXY-005), Shaanxi Province Chinese Medicine Young and Middle-aged Science and Technology Key Talents Project, National Key Talents Project of Traditional Chinese Medicine Clinical Characteristic Technology Inheritance.

Authors' contributions

Study design and conception: Rongqiang Zhang, Yuetong Wang

Data acquisition: Yuetong Wang, Kai Qu

Analysis and interpretation of data: Rongqiang Zhang, Yuetong Wang

All authors read and revised the manuscript, and approved the final version to be published.

Acknowledgments

The authors thank the patients and their families, who have generously donated their organizations to the TCGA, and thank the TCGA members for collecting and disclosing

valuable data.

Authors' information

NA

References

[1] Lin GW, Wang JY, Ge JB. Practice of Internal Medicine. Beijing: People's Medical Publishing House; 2017. 170.

[2] World Health Organization International Agency for Research on Cancer: Latest global cancer data: Cancer burden rises to 19.29 million new cases and 9.96 million cancer deaths in 2020

[3] Zhang J, Wang S, Meng FJ, Yan YJ, Wang B, Guan ZY. Research progress of glutathione peroxidase in tumor. Chinese Journal of Cancer 2019; 38: 282-287.

[4] Jiang YF, Qiu BX, Pang BY, Zhang YF. Research progress on the relationship between GPX3 and tumor and its mechanism. Guangdong Medical Journal 2018; 39: 258-260+265.

[5] Kalatskaya I. Overview of major molecular alterations during progression from Barrett's esophagus to esophageal adenocarcinoma. Ann N Y Acad Sci 2016; 1381: 74–91. https://doi.org/10.1111/nyas.13134

[6] Fujiwara S, Nagai H, Jimbo H, Jimbo N, Tanaka T, Inoie M, et al. Gene Expression and Methylation Analysis in Melanomas and Melanocytes from the Same Patient: Loss of NPM2 Expression Is a Potential Immunohistochemical Marker for Melanoma. Front Oncol 2019; 8: 675. https://doi.org/10.3389/fonc.2018.00675

[7] Hughes DJ, Kunická T, Schomburg L, Liška V, Swan N, Souček P. Expression of Selenoprotein Genes and Association with Selenium Status in Colorectal Adenoma and Colorectal Cancer. Nutrients 2018; 10: 1812. https://doi.org/10.3390/nu10111812

[8] Zhou C, Pan R, Li B, Huang T, Zhao J, Ying J, et al. GPX3 hypermethylation in gastric cancer and its prognostic value in patients aged over 60. Future Oncol 2019; 15: 1279–1289. https://doi.org/10.2217/fon-2018-0674

[9] Worley BL, Kim YS, Mardini J, Zaman R, Leon KE, Vallur PG, et al. GPx3 supports ovarian cancer progression by manipulating the extracellular redox environment. Redox Biol 2019; 25: 101051. https://doi.org/10.1016/j.redox.2018.11.009

[10] Shen SX (2020) Analysis of the expression characteristics of pepsinogen C gene in pan-cancer and its regulatory mechanism. [dissertation/master's thesis]. [Liao Ning]: China Medical University.

[11] Zhang K, Wang H. Cancer Genome Atlas Pan-cancer Analysis Project. Zhongguo Fei Ai Za Zhi 2015; 18:219-23. https://doi.org/10.3779/j.issn.1009-3419.2015.04.02

[12] Ye W, Luo C, Liu F, Liu Z, Chen F. CD96 Correlates with Immune Infiltration and Impacts Patient Prognosis: A Pan-Cancer Analysis. Front Oncol 2021; 11: 634617. https://doi.org/10.3389/fonc.2021.634617

[13] Tang Z, Kang B, Li C, Chen T, Zhang Z. GEPIA2: an enhanced web server for large-scale expression profiling and interactive analysis. Nucleic Acids Res 2019; 47: W556-W560. https://doi.org/10.1093/nar/gkz430

[14] Chen F, Chandrashekar DS, Varambally S, Creighton CJ. Pan-cancer molecular subtypes revealed by mass-spectrometry-based proteomic characterization of more than 500 human cancers. Nat Commun 2019; 10: 5679. https://doi.org/10.1038/s41467-019-13528-0

[15] Cui X, Zhang X, Liu M, Zhao C, Zhang N, Ren Y, et al. A pan-cancer analysis of the oncogenic role of staphylococcal nuclease domain-containing protein 1 (SND1) in human tumors. Genomics 2020; 112: 3958-3967. https://doi.org/10.1016/j.ygeno.2020.06.044

[16] Ju Q, Li XM, Zhang H, Zhao YJ. BRCA1-Associated Protein Is a Potential Prognostic Biomarker and Is Correlated With Immune Infiltration in Liver Hepatocellular Carcinoma: A Pan-Cancer Analysis. Front Mol Biosci 2020; 7: 573619. https://doi.org/10.3389/fmolb.2020.573619

[17] Thorsson V, Gibbs DL, Brown SD, Wolf D, Bortone DS, Ou Yang TH, et al. The Immune Landscape of Cancer. Immunity 2018; 48: 812-830.e14. https://doi.org/10.1016/j.immuni.2018.03.023

[18] Bonneville R, Krook MA, Kautto EA, Miya J, Wing MR, Chen HZ, et al. Landscape of Microsatellite Instability Across 39 Cancer Types. JCO Precis Oncol 2017; 2017: PO.17.00073. https://doi.org/10.1200/PO.17.00073

[19] Pan JH, Zhou H, Cooper L, Huang JL, Zhu SB, Zhao XX, et al. LAYN Is a Prognostic Biomarker and Correlated With Immune Infiltrates in Gastric and Colon Cancers. Front Immunol 2019; 10: 6. https://doi.org/10.3389/fimmu.2019.00006

[20] Wang Z, Gao L, Guo X, Feng C, Lian W, Deng K, et al. Development and validation of a nomogram with an autophagy-related gene signature for predicting survival in patients with glioblastoma. Aging (Albany NY) 2019; 11: 12246-12269. https://doi.org/10.18632/aging.102566

[21] Chen L, Long C, Liu J, Duan X, Xiang Z. Prognostic nomograms to predict overall survival and cancer-specific survival in patients with pelvic chondrosarcoma. Cancer Med 2019; 8: 5438-5449. https://doi.org/10.1002/cam4.2452

[22] Chang QH, Mao T, Tao Y, Dong T, Tang XX, Ge GH, et al. Pan-cancer analysis identifies *ITIH1* as a novel prognostic indicator for hepatocellular carcinoma. Aging (Albany NY) 2021; 13:11096-11119. https://doi.org/10.18632/aging.202765

[23] Chen M, Zhang S, Nie Z, Wen X, Gao Y. Identification of an Autophagy-Related Prognostic Signature for Clear Cell Renal Cell Carcinoma. Front Oncol 2020;10: 873. https://doi.org/10.3389/fonc.2020.00873

[24] Saelee P, Pongtheerat T, Sophonnithiprasert T. Reduced Expression of GPX3 in Breast Cancer Patients in Correlation with Clinical Significance. Glob Med Genet 2020; 7: 87-91. https://doi.org/10.1055/s-0040-1722170

[25] Lou W, Ding B, Wang S, Fu P. Overexpression of GPX3, a potential biomarker for diagnosis and prognosis of breast cancer, inhibits progression of breast cancer cells in vitro. Cancer Cell Int 2020; 20: 378. https://doi.org/10.1186/s12935-020-01466-7

[26] Noci S, Dugo M, Bertola F, Melotti F, Vannelli A, Dragani TA, et al. A subset of genetic susceptibility variants for colorectal cancer also has prognostic value. Pharmacogenomics J 2016; 16: 173-9. https://doi.org/10.1038/tpj.2015.35

[27] Li HL, Yu W, Chen YT, Li J. Changes of serum Gal-1 and GPX3 expression in patients with thyroid cancer and their relationship with disease severity 2020; 22: 191-193.

[28] Wang Y, Zhang WY, Han QW, Liu Y, Dai HR, Guo YL, et al. Effective response and delayed toxicities of refractory advanced diffuse large B cell lymphoma treated by CD20 directed chimeric antigen receptor modified T cells. Clin Immunol 2014; 155: 160-175. https://doi.org/10.1016/j.clim.2014.10.002

[29] Qu Y, Dang S, Hou P. Gene methylation in gastric cancer. Clin Chim Acta 2013; 424: 53-65. https://doi.org/10.1016/j.cca.2013.05.002

[30] An BC, Choi YD, Oh IJ, Kim JH, Park JI, Lee SW. GPx3-mediated redox signaling arrests the cell cycle and acts as a tumor suppressor in lung cancer cell lines. PLoS One 2018; 13: e0204170. https://doi.org/10.1371/journal.pone.0204170

[31] Cai M, Sikong Y, Wang Q, Zhu S, Pang F, Cui X. Gpx3 prevents migration and invasion in gastric cancer by targeting NFκB/Wnt5a/JNK signaling. Int J Clin Exp Pathol 2019; 12:1194-1203.

[32] Chang C, Worley BL, Phaëton R, Hempel N. Extracellular Glutathione Peroxidase GPx3 and Its Role in Cancer. Cancers (Basel) 2020; 12: 2197. https://doi.org/10.3390/cancers12082197

[33] Miess H, Dankworth B, Gouw AM, Rosenfeldt M, Schmitz W, Jiang M, et al. The glutathione redox system is essential to prevent ferroptosis caused by impaired lipid metabolism in clear cell renal cell carcinoma. Oncogene 2018; 37:5435-5450. https://doi.org/10.1038/s41388-018-0315-z

[34] Lee HJ, Do JH, Bae S, Yang S, Zhang X, Lee A, et al. Immunohistochemical evidence for the over-expression of Glutathione peroxidase 3 in clear cell type ovarian adenocarcinoma. Med Oncol 2011;28 Suppl 1: S522-7. https://doi.org/10.1007/s12032-010-9659-0

[35] Pelosof L, Yerram S, Armstrong T, Chu N, Danilova L, Yanagisawa B, et al. GPX3 promoter methylation predicts platinum sensitivity in colorectal cancer. Epigenetics 2017; 12: 540-550. https://doi.org/10.1080/15592294.2016.1265711

Figures

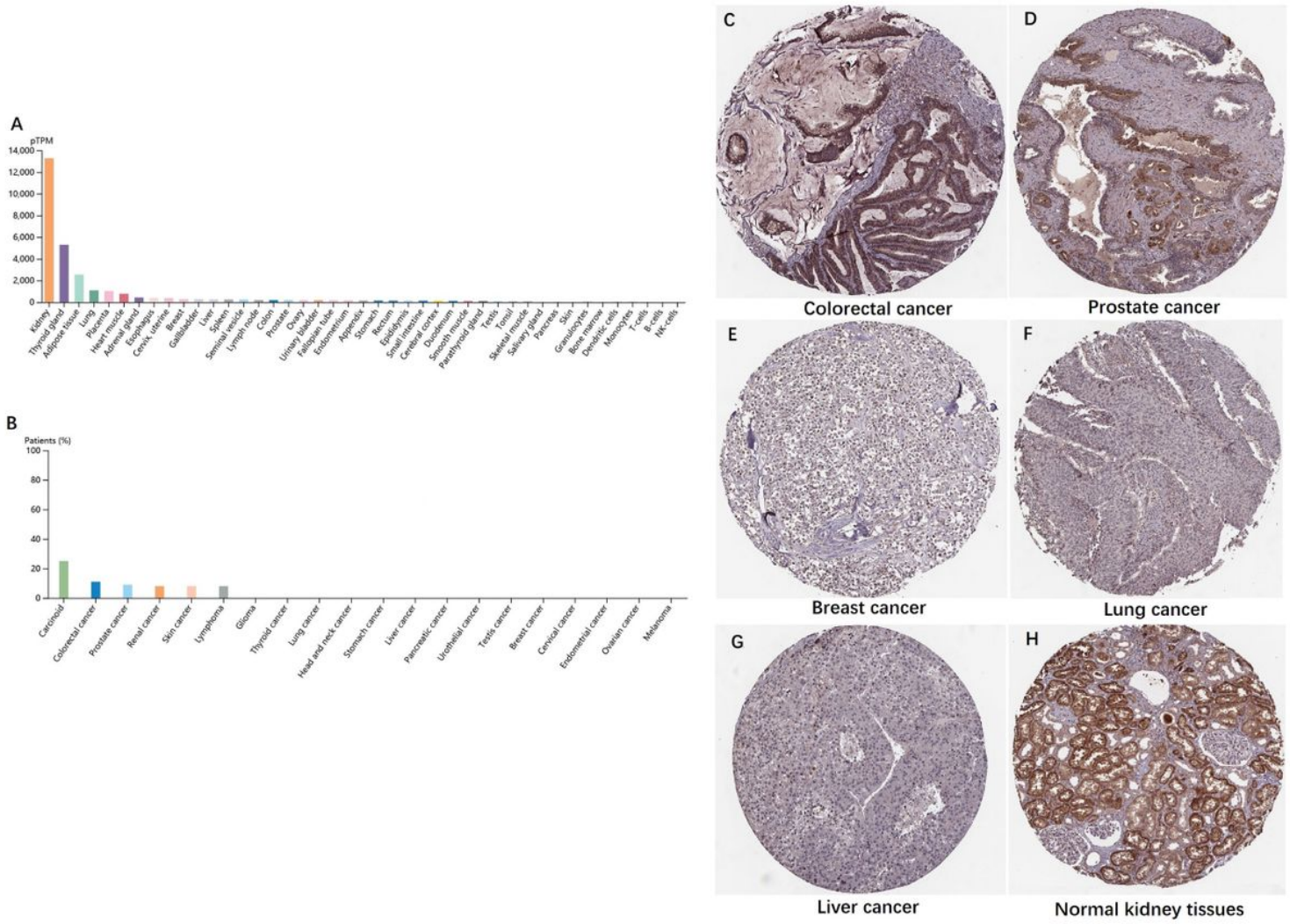

Figure 1

Expression profiles of GPX3 in normal and cancer tissues. (A) The mRNA level of GPX3 in normal human tissues [Y-axis means protein-coding transcripts per million (pTPM); X-axis means normal human tissue]. (B) Detection rate of GPX3 protein in human tumor tissues. (C-H) Representative IHC images showing GPX3 expression in colorectal cancer, prostate cancer, breast cancer, lung cancer, liver cancer and normal kidney tissues.

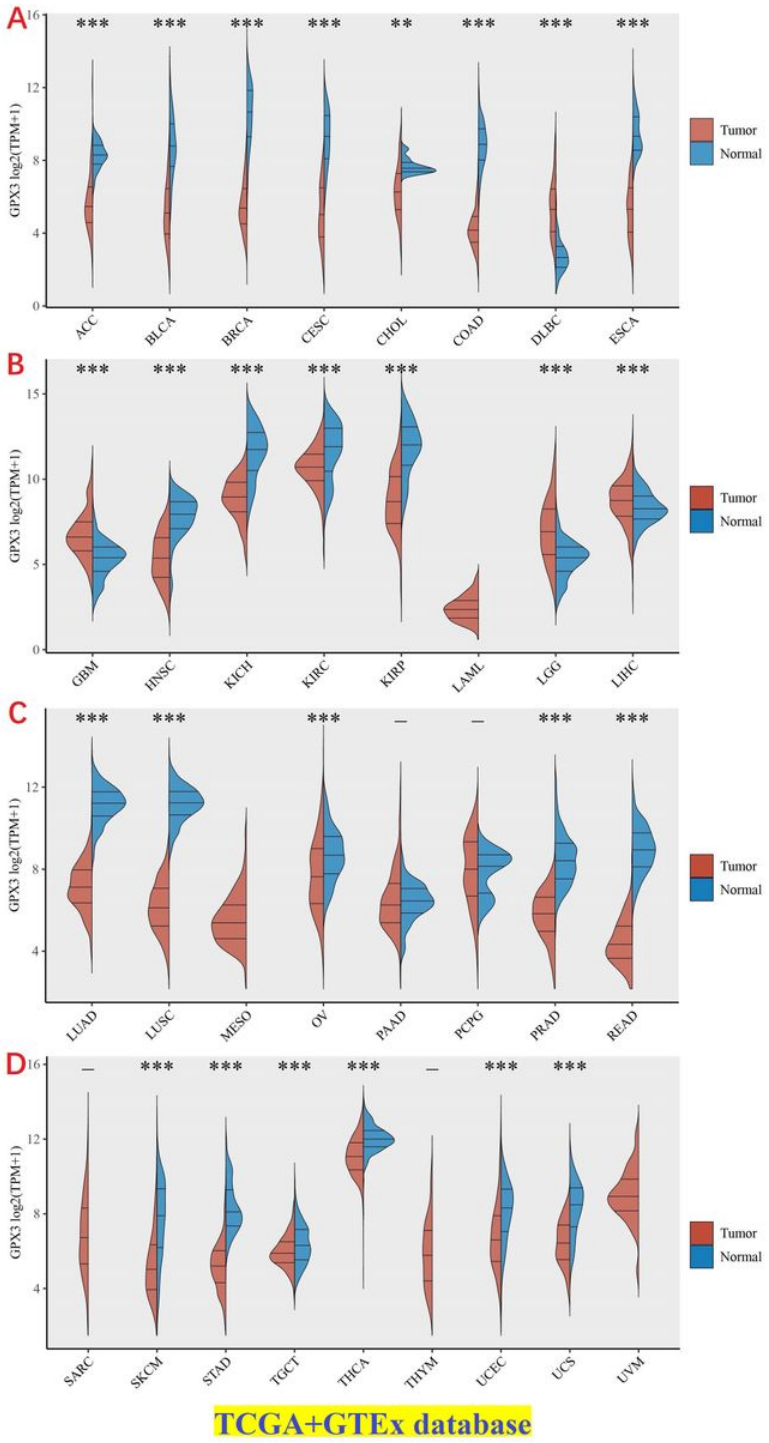

Figure 2

Expression level of GPX3 gene in different cancers from TCGA+GTEx database (*P<0.05；**P<0.01；***P<0.001)

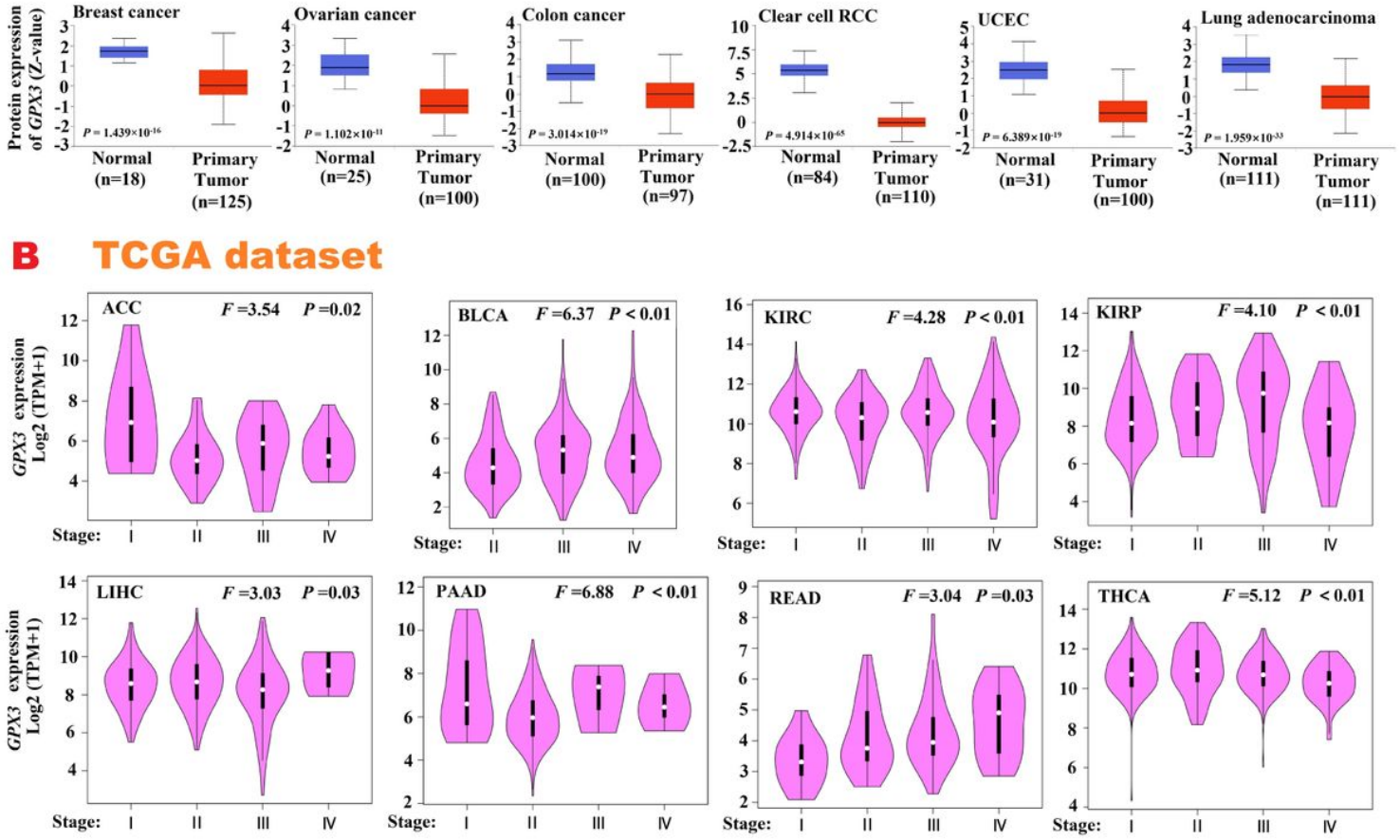

Figure 3

GPX3 expression level in different cancers (A) Expression level of GPX3 total protein in normal tissues and primary tumors of breast cancer, ovarian cancer, colon cancer, clear cell RCC, UCEC, lung adenocarcinoma. (B) Expression level of GPX3 in the main pathological stages of ACC, BLCA, KIRC, KIRP, LIHC, PAAD, READ and THCA.

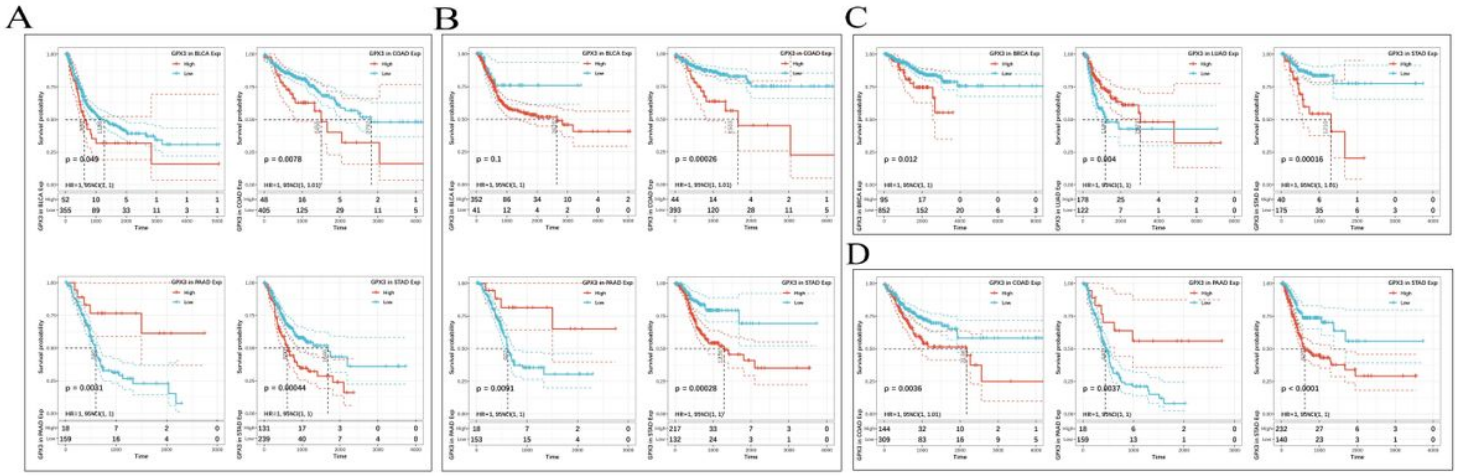

Figure 4

Kaplan-Meier curves reflect the prognostic value of GPX3 in different cancers (A) OS of patients in BLCA, COAD, PAAD and STAD with low or high GPX3 (B) DSS of patients in BLCA, COAD, PAAD and STAD with low or high GPX3. (C) Kaplan–Meier DFI curves for patients stratified by different expression levels of GPX3 in BLCA, LUAD and STAD. (D) PFI of patients in COAD, PAAD and STAD with low or high GPX3.

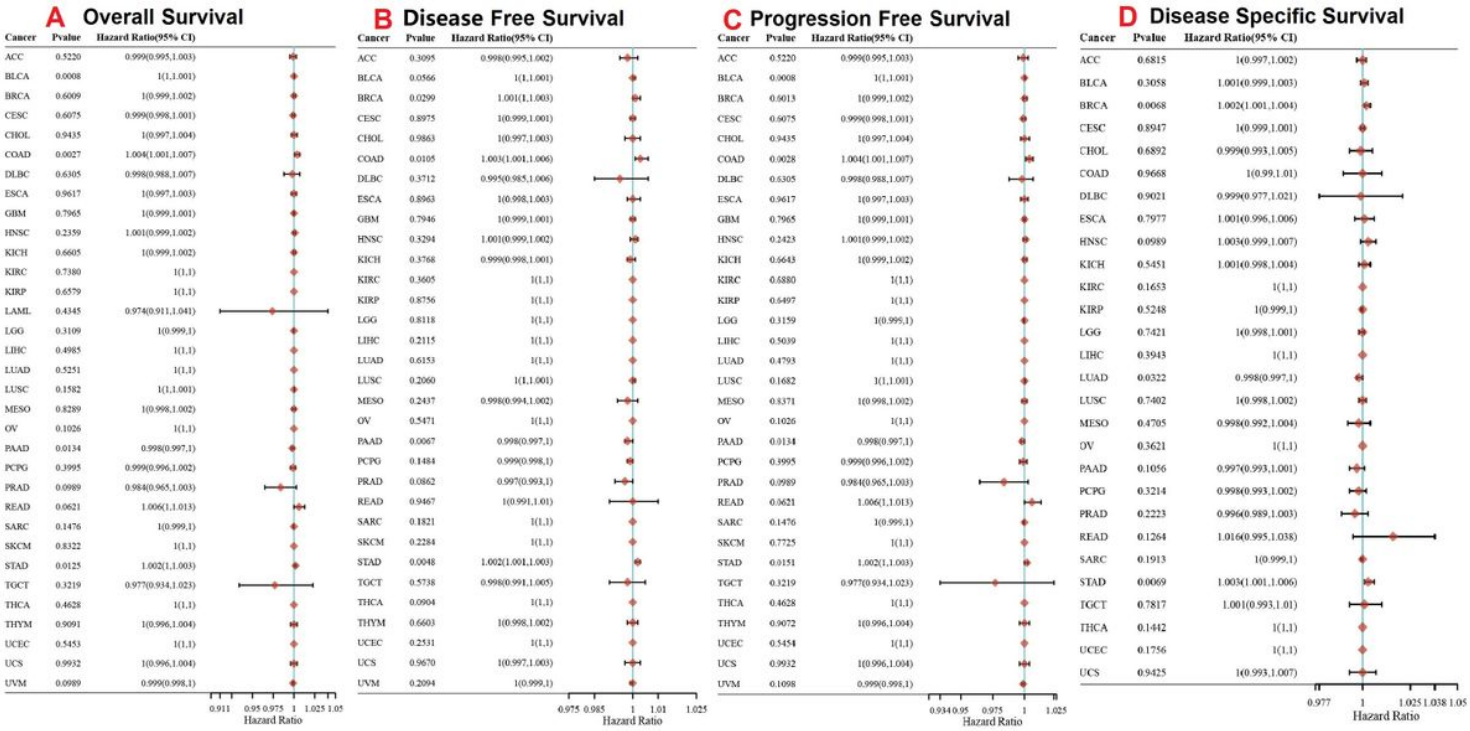

Figure 5

Correlation of GPX3 gene expression with patient's OS, DFS, PFS and DSS in different cancer types. The forest plots with the hazard ratios (HR) and 95% confidence intervals for OS, DFS, PFS and DSS in different cancers showing the survival advantage and disadvantage of low expression of GPX3. (HR>1, indicates that high GPX3 expression predicts worse prognosis compared to low GPX3 expression, whereas HR<1 indicates that high GPX3 expression predicts better prognosis than low GPX3 expression)

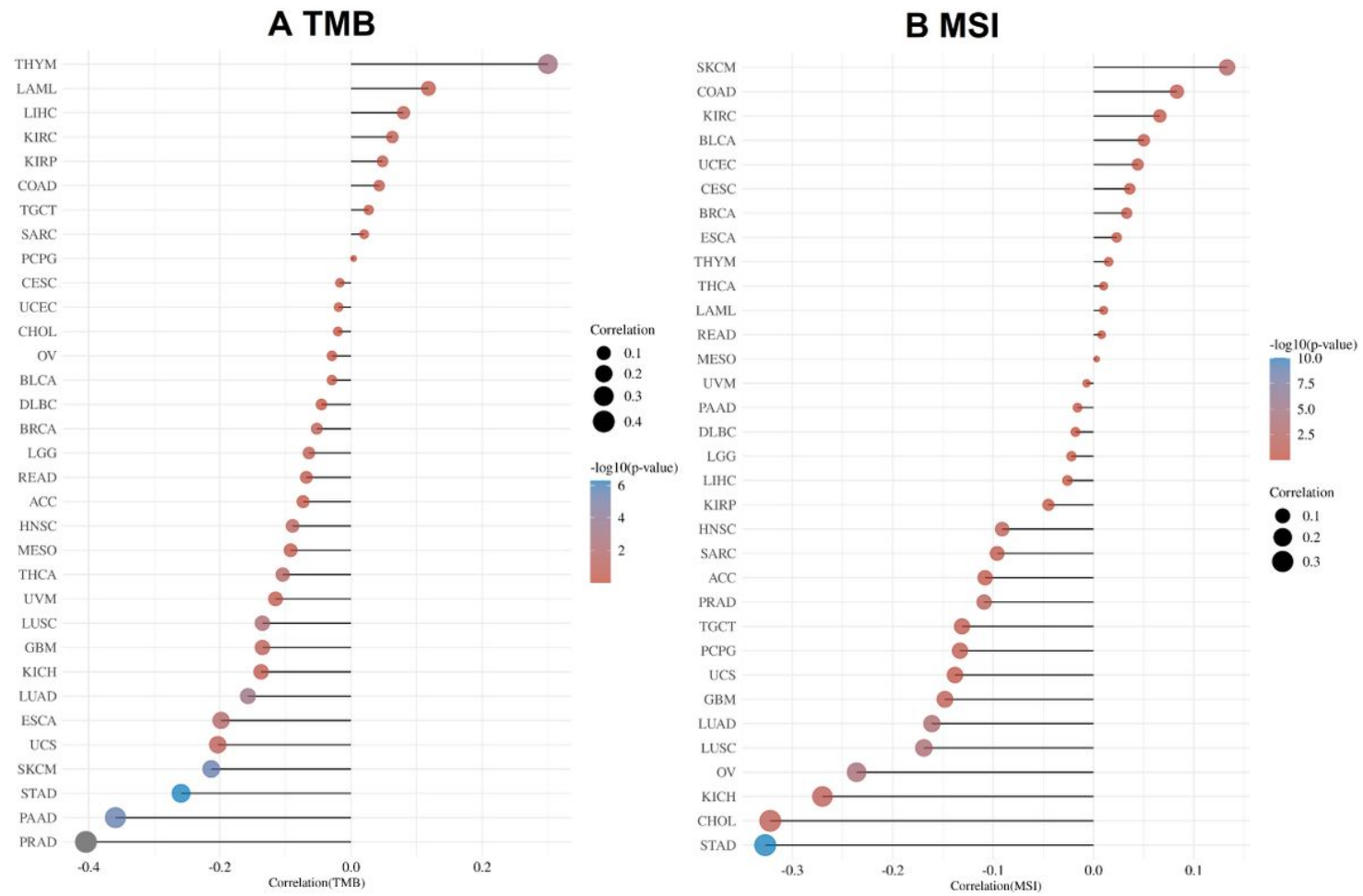

Figure 6

Mutation profiles of GPX3 in different cancers from the TCGA (A) Spearman correlation analysis showing the association between TMB and GPX3 gene expression (B) Spearman correlation analysis showing the correlation between MSI and GPX3 gene expression (The X-axis represents the correlation coefficient between genes and TMB/MSI, while the Y-axis represents different tumors. The size of dots in the figure represents the correlation coefficient, and different colors represent the significance of P value. In the schematic diagram, the redder the color, the smaller the P value)

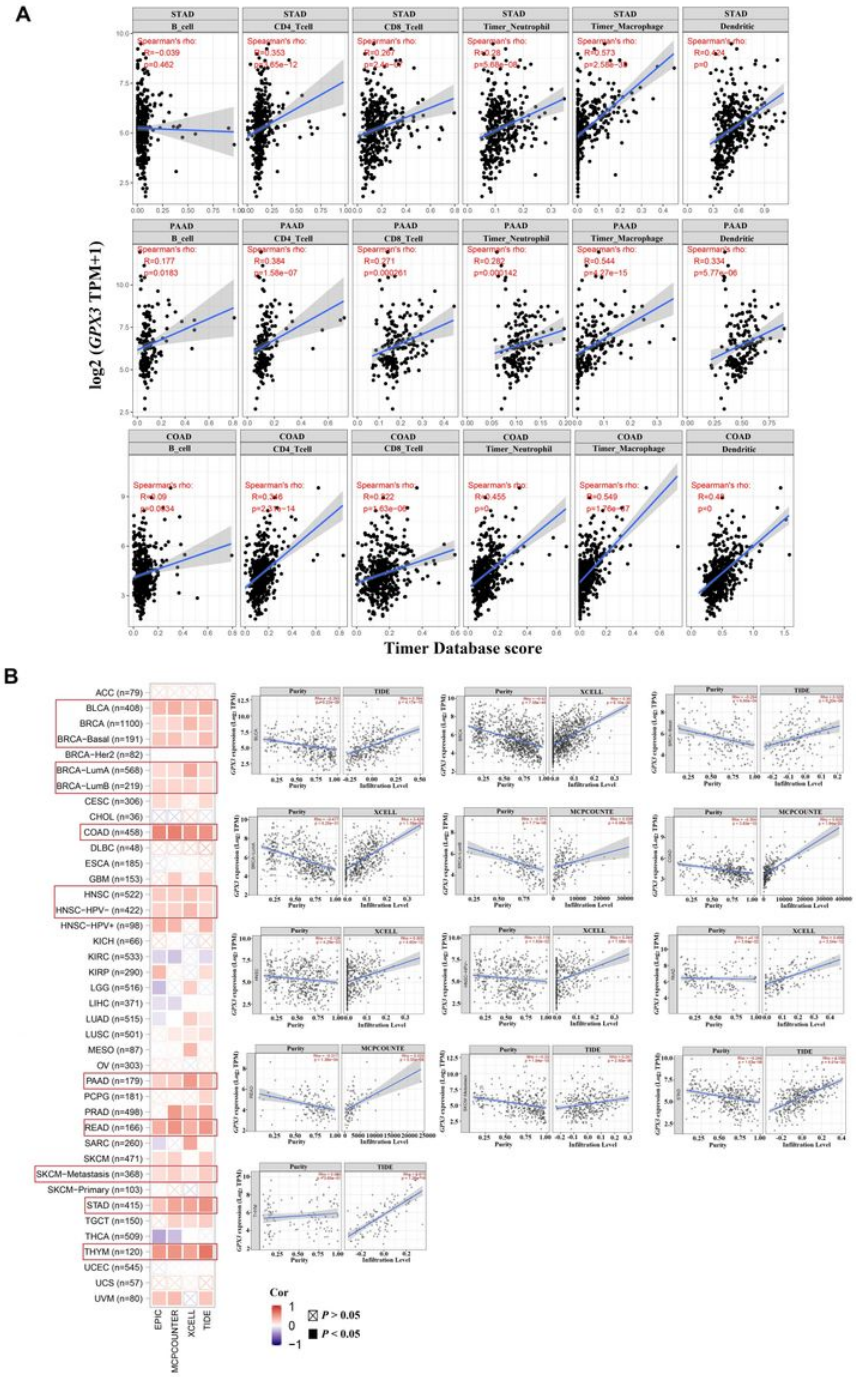

Figure 7

Correlation analysis between GPX3 expression and immune infiltration (A) Correlation between GPX3 expression and the level of STAD, PAAD and COAD immune infiltration (B) Correlation between the expression of GPX3 and immune infiltration of CAFs.

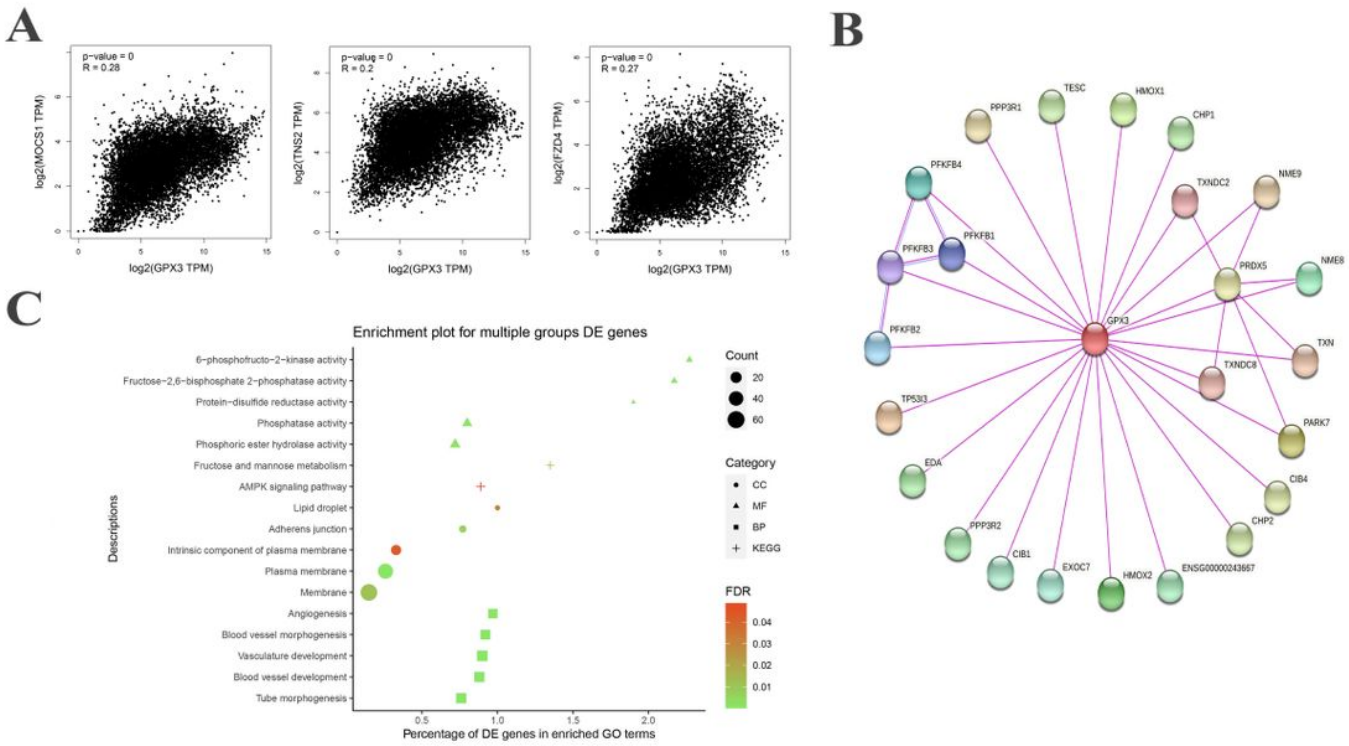

Figure 8

Enrichment gene associated with GPX3 (A) The correlation between GPX3 and the top 3 similarly expressed genes (B) A protein-protein interaction network for GPX3 (C) The results of enrichment analysis for GPX3 in different human tumors.

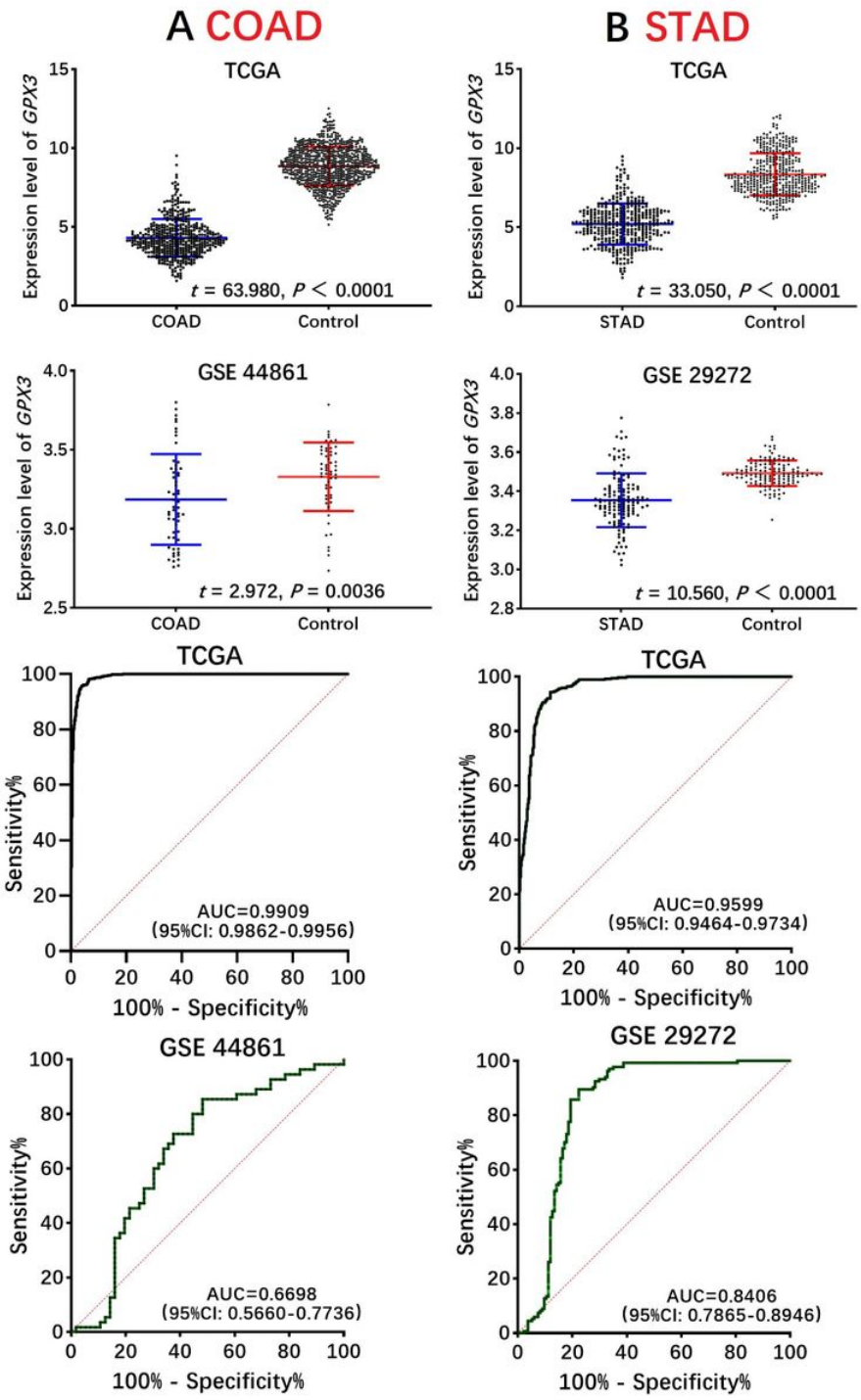

Figure 9

Independent validation of the differential expression and prognostic significance of GPX3 in GEO and TCGA datasets (A) the differential expression and prognostic significance of GPX3 in COAD (B) the differential expression and prognostic significance of GPX3 in STAD

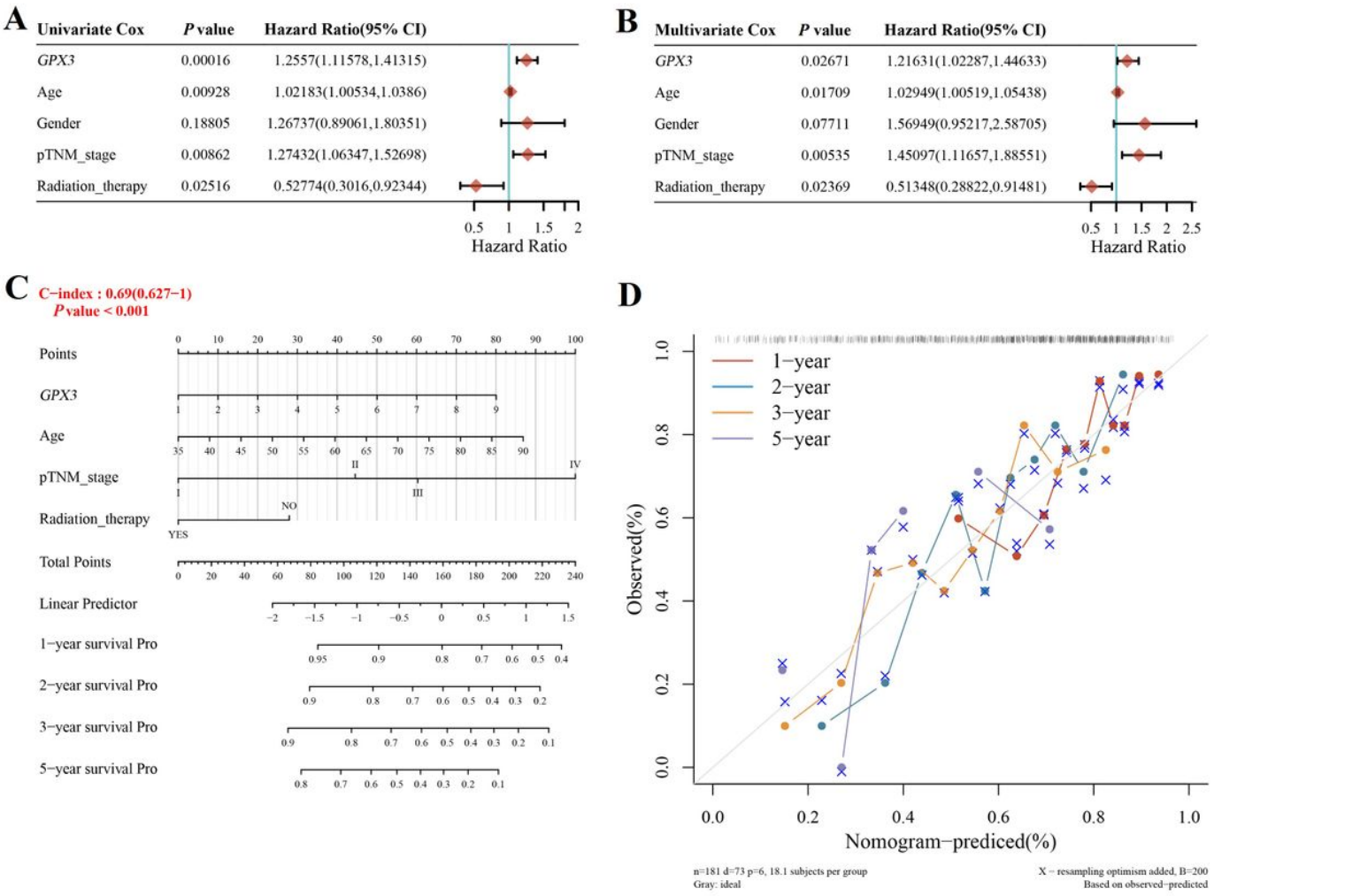

Figure 10

The nomogram predicted the probability survival in patients with STAD (A, B) Univariate and multivariate Cox proportional risk analyses of clinical parameters and risk scores in patients with STAD in the TCGA training cohort and CGGA validation cohort (C) Prognostic nomogram including age, pTNM stage and radiation therapy assessed probability survival of 1-, 2-, 3- and 5- years (D) The calibration curves of the nomogram predicted survival in patients with STAD.